J Appl Electrochem (2010) 40:209–213
DOI 10.1007/s10800-009-9958-3

SHORT COMMUNICATION

$LiVOPO_4$ as an anode material for lithium ion batteries

M. M. Ren · Z. Zhou · X. P. Gao

Received: 26 March 2009 / Accepted: 9 June 2009 / Published online: 18 June 2009

Abstract β-$LiVOPO_4$ was prepared via a sol–gel method and exploited as an anode material for lithium ion batteries. The β-$LiVOPO_4$ anode material showed a reversible capacity higher than 380 mAh g^{-1} during 30 cycles; the coulombic efficiency exceeded 94%. We speculated a conversion reaction mechanism for Li recycle, $VPO_4 + 3Li^+ + 3e^- \leftrightarrow V + Li_3PO_4$. The higher discharge capacity and cyclic ability may be due to the large ${PO_4}^{3-}$ ions that can alleviate the change of the cell volume during the charge/discharge processes, and the formation of Li_2O during the first discharge process that can buffer the volume change in the electrodes.

Keywords Li ion batteries · Anode material · Mechanism · β-$LiVOPO_4$ · Sol–gel method

1 Introduction

Graphite-based materials are used as anodes for lithium ion batteries, since the commercialization in early 1990s; however, these materials have lower theoretical capacity (372 mAh g^{-1}) [1]. Metal oxides and alloys are the most widely investigated alternative anode materials for lithium ion batteries with high theoretical capacity, whereas the large volume variation during charge/discharge processes severely affects the cyclic stability [2, 3]. Therefore, it is necessary to search for new anode candidates for lithium ion batteries.

Transition metal phosphates exhibit remarkable electrochemical and thermal stability as well as comparable energy density, and have been attracting much interest as a new class of cathode materials for lithium ion batteries [4–10]. Recently, Kalaiselvi et al. have proposed that $LiFePO_4$ could also be used as an anode material for lithium ion batteries, and presented higher specific capacity than that of $LiFePO_4$ used as a cathode material [11].

In search for polyanion insertion hosts, lithium vanadyl phosphate ($LiVOPO_4$) is also a candidate [12–16]. $LiVOPO_4$ contains two crystal phases, α- and β-$LiVOPO_4$, and both $LiVOPO_4$ phases can be used as cathode materials for lithium ion batteries [9, 13, 17]. Can β-$LiVOPO_4$ also be used as an anode material for lithium ion batteries as $LiFePO_4$? How are its electrochemical performance and cyclic stability? What is the mechanism for Li recycle during charge/discharge processes in this material? In this study, we prepared β-$LiVOPO_4$ and investigated its electrochemical performance as an anode material for Li ion batteries to address the above questions.

2 Experimental

2.1 Preparation of β-$LiVOPO_4$

β-$LiVOPO_4$ was prepared through a sol–gel route [18]. Starting materials were V_2O_5, $LiNO_3{\cdot}6H_2O$, $NH_4H_2PO_4$ and oxalic acid. Firstly, oxalic acid (3.02 g) and V_2O_5 (1.46 g) were dissolved in 80 ml deionized water with magnetic stirring at 70 °C. After a clear blue solution formed, a mixture of $NH_4H_2PO_4$ (1.84 g) and $LiNO_3{\cdot}6H_2O$ (1.16 g) was added to the solution while stirring for 4 h, and then a gel formed in an air oven at 100 °C. Finally, the

---

M. M. Ren · Z. Zhou (✉) · X. P. Gao
Institute of New Energy Material Chemistry,
Nankai University, Tianjin 300071, China
e-mail: zhouzhen@nankai.edu.cn

gel was decomposed at 300 °C for 4 h, and the obtained product was sintered at 500 °C for 4 h in air.

2.2 Sample characterization

X-ray diffraction (XRD) patterns were measured under the D/MAX Ⅲ diffractometer with Cu $K\alpha$ radiation ($\lambda = 1.5418$ Å). The morphologies were observed through a Hitachi S-3500 N scanning electron microscopy (SEM).

2.3 Galvanostatic charge/discharge tests

Electrochemical performances of the samples were evaluated in Li test cells. The anodes were prepared by mixing the samples with acetylene black and polytetrafluoroethylene (PTFE) with a weight ratio of 75:20:5 in ethanol to ensure homogeneity. After ethanol was evaporated, the mixture was rolled into a sheet, and the sheet was cut into circular strips of 8 mm in diameter. The strips were then dried at 100 °C for 10 h. Lithium metal was used as the reference and counter electrode. The electrolyte was composed of a 1 mol l^{-1} $LiPF_6$ dissolved in ethylene carbonate (EC)/dimethyl carbonate (DMC)/ethylene methyl carbonate (EMC) with the volume ratio of 1:1:1. Test cells were assembled in an argon-filled dry glove box. The galvanostatic charge/discharge tests were performed with a Land CT2001 battery tester at the current density of 20 mA g^{-1} in a potential range of 3.5–0.01 V at 25 °C.

2.4 Cyclic voltammograms

Cyclic voltammograms (CVs) were conducted within a CHI 600A electrochemical analyzer. The CV curves were recorded for the test cells in a potential range of 3.5–0.01 V (vs. Li^+/Li) with the scan rate of 0.2 mV/s at 25 °C.

3 Results and discussion

3.1 Sample characterization

XRD pattern of β-$LiVOPO_4$ is shown in Fig. 1. β-$LiVOPO_4$ possesses an orthorhombic symmetry with the space group, *Pnma*. The reflections are indexed with JCPDS (No. 85-2438). There are two impurity peaks at 27.2° and 29.7°, ascribed to α-$LiVOPO_4$ (JCPDS No. 72-2253).

The surface morphology of β-$LiVOPO_4$ was investigated through SEM. As seen in the SEM image in Fig. 2, the sample consists of uniform particles with average sizes of ~2 μm.

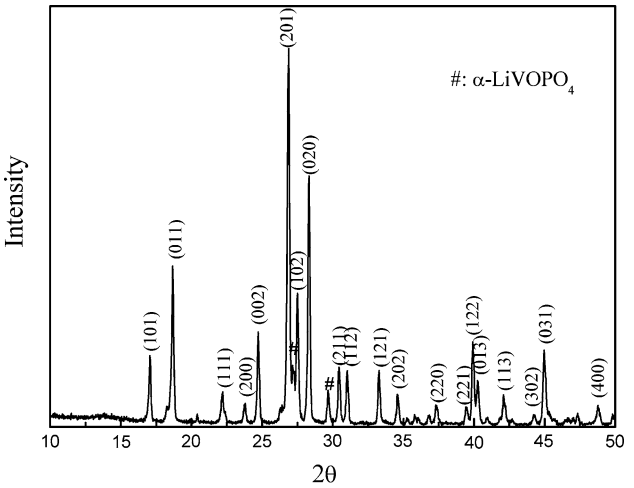

Fig. 1 XRD pattern of β-$LiVOPO_4$ prepared through the sol–gel route

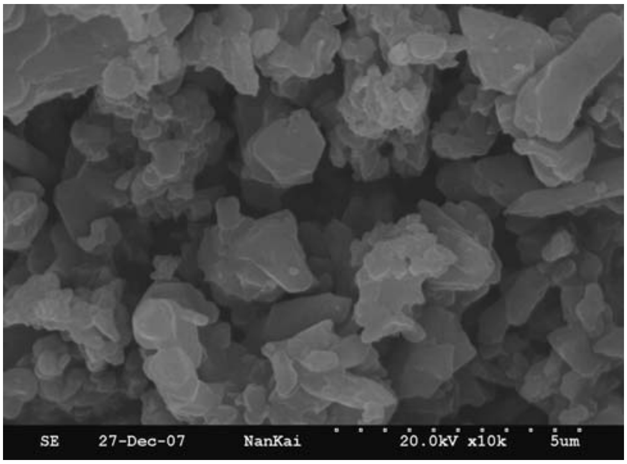

Fig. 2 SEM image of β-$LiVOPO_4$ synthesized through the sol–gel route

3.2 Galvanostatic charge/discharge tests

The galvanostatic charge/discharge performances of β-$LiVOPO_4$ as an anode material are exhibited in Fig. 3a. There is a plateau around 2.1 V during the first discharge curve, which corresponds to one Li^+ insertion associated with the V^{3+}/V^{4+} redox couple [19]. However, this phenomenon is not seen from the subsequent charge/discharge curves; therefore, the initial charge/discharge process of β-$LiVOPO_4$ is not reversible. As an anode material, the sample shows high discharge capacity; the initial charge and discharge capacities are 417.0 and 725.5 mAh g^{-1}, respectively. The irreversible capacity is 308.5 mAh g^{-1}, due to the irreversible change between V^{3+}/V^{4+} redox couple and the formation of the solid electrolyte interphase (SEI) film [20, 21]. However, the irreversible capacity reduces to

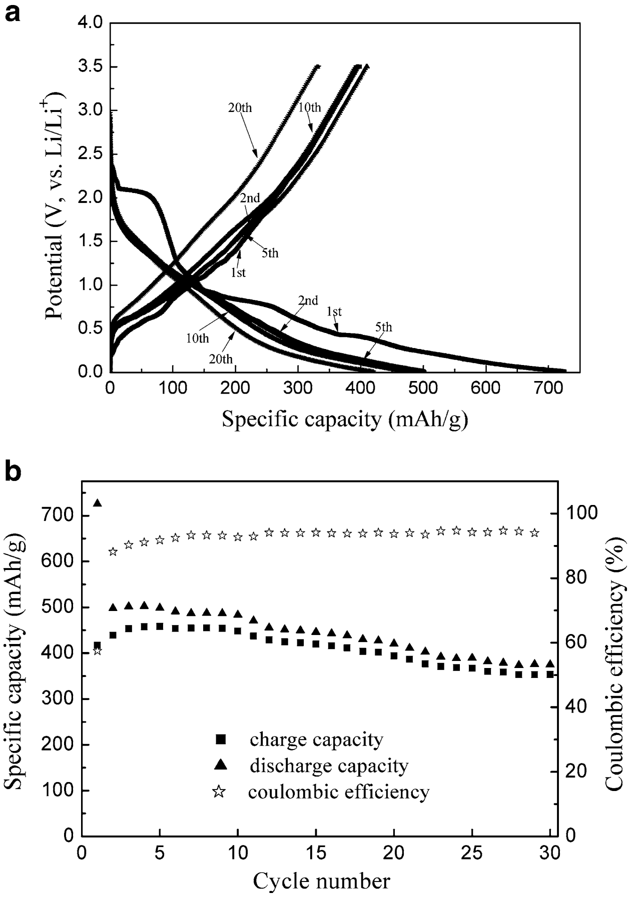

Fig. 3 Electrochemical performances of β-LiVOPO$_4$ as an anode material in Li ion batteries tested at 20 mA/g in the potential range of 0.01 ~ 3.5 V at 25 °C: **a** galvanostatic charge/discharge curves and **b** cyclic performance

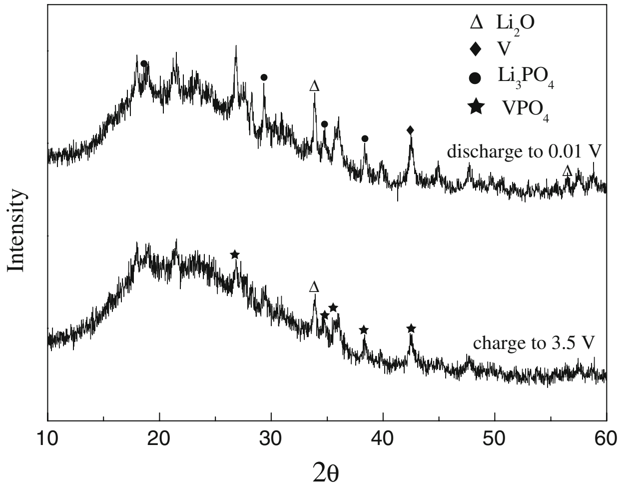

Fig. 4 XRD patterns of the β-LiVOPO$_4$ electrode during the first cycle at charged state (3.5 V) and discharged state (0.01 V)

58.7 mAh g^{-1} in the second cycle. The discharge capacities for the 2nd, 10th, and 20th cycles are 497.0, 487.0, and 427.0 mAh g^{-1}, respectively, and the discharge capacity retention rate is 75.5% from the 2nd to the 30th cycle. In addition, β-LiVOPO$_4$ anode material shows coulombic efficiency higher than 90% after the second cycle, as shown in Fig. 3b, especially upon progressive cycling.

3.3 Lithium storage mechanism

In order to get insight into the electrochemical mechanism of lithium storage in β-LiVOPO$_4$ electrode, XRD patterns were taken for the specimens from the electrode at the charged state (3.5 V) and discharged state (0.01 V), and are presented in Fig. 4. Three phases, Li$_3$PO$_4$, V, and Li$_2$O, were mainly detected at the discharged state; and mainly two phases, Li$_2$O and VPO$_4$, were observed at the charged state. Therefore, we can propose the lithium recycle process in β-LiVOPO$_4$. As mentioned above, there is a plateau around 2.1 V in the first discharge curve, which corresponds to one lithium insertion associated with the V^{3+}/V^{4+} redox couple (Eq. 1). Another three lithium ions can enter the network of Li$_2$VOPO$_4$ and react with it to form Li$_3$PO$_4$, V, and Li$_2$O when the electrode is discharged to 0.01 V (Eq. 2). In the charging process, V can react with Li$_3$PO$_4$ (Eq. 3), and then during the subsequent cycles, lithium is reversibly cycled with the material network, as described in Eq. 3. Ouyang et al. reported that Li$_3$FePO$_4$ possessed a stable structure after lithium is intercalated into the LiFePO$_4$ host when it was used as an anode material through theoretical computations [22]. The valence of Fe is 0 in Li$_3$FePO$_4$; it can be regarded as Li$_3$PO$_4$ and Fe, and the reversible reaction process may be $\mathrm{Fe} + \mathrm{Li_3PO_4} \leftrightarrow \mathrm{FePO_4} + 3\mathrm{Li^+} + 3\mathrm{e^-}$, in agreement with our proposal.

$$\mathrm{LiVOPO_4} + \mathrm{Li^+} + \mathrm{e^-} \rightarrow \mathrm{Li_2VOPO_4} \qquad (1)$$

$$\mathrm{Li_2VOPO_4} + 3\mathrm{Li^+} + 3\mathrm{e^-} \rightarrow \mathrm{Li_2O} + \mathrm{Li_3PO_4} + \mathrm{V} \qquad (2)$$

$$\mathrm{V} + \mathrm{Li_3PO_4} \leftrightarrow \mathrm{VPO_4} + 3\mathrm{Li^+} + 3\mathrm{e^-} \qquad (3)$$

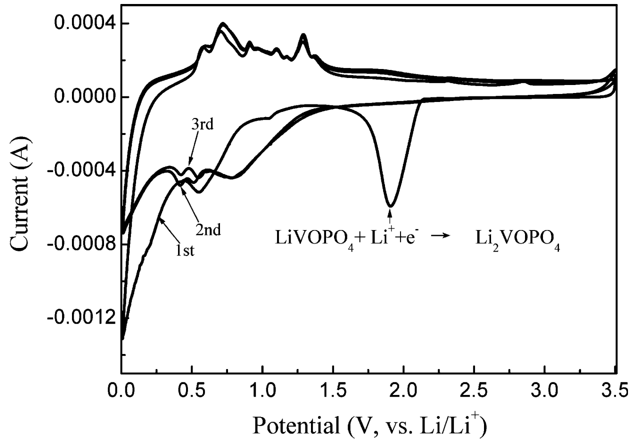

Fig. 5 CV curves of the β-LiVOPO$_4$ electrode tested at the scan rate of 0.2 mV/s in the potential range of 0.01–3.5 V

From the above discussion, we can see that Eq. 3 is the main reaction for the anode material in the subsequent charge/discharge cycles. The theoretical potential of Eq. 3, which we can get from the charge-discharge curves is below 1.5 V, and the theoretical reversible capacity of Eq. 3 is about 551 mAh g^{-1}, derived from the maximum uptake of 3Li's to VPO_4 based the above mechanism. During the initial discharge, there are three inclined discharge plateaus; however, these plateaus disappeared from the second cycle, which was also found in transition metal oxides as anode materials. The phenomena may result from the facts that the processes after the initial discharge are conversion reactions [23] (not insertion reactions) involving multi-electrons. The decomposition of the electrolyte and the formation of SEI film account mostly for the excess capacity of the first cycle [21], and here for β-$LiVOPO_4$ material the first irreversible lithium insertion also contributes to the excess initial discharge capacity.

3.4 CV measurements

Typical CV curves of β-$LiVOPO_4$ as an anode material are depicted in Fig. 5. The main cathodic peak located around 2.0 V vs. Li/Li^+ in the initial cycle, corresponding to the first lithium insertion; however, the peak disappears in the subsequent cycles, indicating that this process is irreversible, which is in agreement with the initial discharge curve (Fig. 3a). In the second and third cycles, the CV curves are different from the initial one, illustrating the different lithium reaction processes. The cathodic peaks and anodic peaks between 1.5 and 0.2 V may be related to the process as described in Eq. 3. In Fig. 5, we can also see that the CV curves of the second cycle and the third cycle are nearly the same, indicating that the anode material has good reversibility in the subsequent cycles.

The β-$LiVOPO_4$ anode material exhibits high discharge capacity and acceptable cyclic capability. β-$LiVOPO_4$ has similar lithium storage mechanism ($V + Li_3PO_4 \leftrightarrow VPO_4 + 3Li^+ + 3e^-$), to transition metal oxides: $yLi_2O + xM \leftrightarrow M_xO_y + 2yLi^+ + 2ye^-$ [24]. Large polyanions instead of the smaller O^{2-} ions increase the molar weight and decrease the theoretical capacity accordingly; hence, β-$LiVOPO_4$ has lower initial charge/discharge capacities than transition metal oxide anode materials; however, the large polyanions build an open 3D framework which can help to stabilize the structure and may alleviate the change of the cell volume during the charge and discharge process; therefore, β-$LiVOPO_4$ showed better cyclic performance than transition metal oxide anode materials. Through the above results, we can see that β-$LiVOPO_4$ has higher initial discharge capacity (725.5 mAh g^{-1}) than $LiFePO_4$ (610 mAh g^{-1}) because $LiFePO_4$ has no Li_2O formation during the initial discharge process [11]. Also, β-$LiVOPO_4$ has better cyclic performance than $LiFePO_4$ due to the presence of Li_2O which serves as a matrix and buffers the volume change in the electrode.

4 Conclusion

Orthorhombic β-$LiVOPO_4$ has been prepared and investigated systematically as an anode material for lithium ion batteries. This anode material exhibits higher discharge capacity and acceptable cyclic capability. Large PO_4^{3-} can stabilize the structure and may alleviate the change of the cell volume during the charge and discharge process and the formation of Li_2O during the first discharge process can buffer the volume changes in the electrode. Hence, $LiVOPO_4$ may be exploited as an anode material for lithium ion batteries in the future.

Acknowledgments This work was supported by the 863 National High Technology Research and Development Program (2007AA03Z225), the 973 National Basic Research Program (2009CB220100), and Tianjin Natural Science Foundation (06YFJMJC13300) in China.

References

1. Rougier A, Graveau P, Delama C (1999) J Electrochem Soc 146:1168
2. Poizot P, Laruelle S, Grugeon S et al (2000) Nature 407:496
3. Winter M, Besenhard JO (1999) Electrochem Acta 45:31
4. Padhi AK, Najundaswamy KS, Goodenough JB (1997) J Electrochem Soc 144:1188
5. Amine K, Yamachi K, Yamachi M (2000) Electrochem Solid State Lett 3:A178
6. Saidi MY, Barker J, Huang H et al (2003) J Power Sources 119–112:266
7. Yin SC, Grond H, Strobel P et al (2003) J Am Chem Soc 125:326
8. Hung H, Yin SC, Kerr T et al (2002) Adv Mater 14:1525
9. Ren MM, Zhou Z, Gao XP et al (2008) J Phys Chem C 112:5689
10. Li YZ, Zhou Z, Gao XP et al (2006) J Power Sources 160:633
11. Kalaiselvi N, Doh C-H, Park C-W et al (2004) Electrochem Comm 6:1110
12. Ganbicher J, Mercier TL, Chahre Y et al (1999) J Electrochem Soc 146:4375
13. Barker J, Saidi MY, Swoyer JL (2004) J Electrochem Soc 151:A796
14. Azmi BM, Ishihara T, Nishiguchi H et al (2002) Electrochem Acta 48:165
15. Kerr TA, Gaubicher J, Nazar LF (2000) Electrochem Solid State Lett 3:460
16. Dupre N, Gaubicher J, Mercier TL et al (2001) Solid State Ion 140:209
17. Ren MM, Zhou Z, Gao XP et al (2008) J Phys Chem C 112:13043
18. Ren MM, Zhou Z, Su LW et al (2009) J Power Sources 189:786
19. Patoux S, Wurm C, Morcrette M et al (2003) J Power Sources 119–121:278
20. Zhu JJ, Lu ZH, Aruna ST et al (2000) Chem Mater 12:2557

21. Rong A, Gao XP, Li GR et al (2006) J Phys Chem B 110:14754
22. Ouyang CY, Shi SQ, Fang Q et al (2008) J Power Sources 175:891
23. Armand M, Tarascon J-M (2008) Nature 451:652
24. Huang XH, Tu JP, Zhang CQ et al (2007) Electrochem Comm 9:1180